symmetry

MDPI

Article

Impact of Inertial Forces on Car Occupants in a Vehicle-Fixed Barrier Front Crash

Stanimir Karapetkov, Hristo Uzunov, Silvia Dechkova * and Vasil Uzunov

Faculty of Engineering and Pedagogy, Technical University of Sofia, 1000 Sofia, Bulgaria; skarapetkov@tu-sofia.bg (S.K.); huzunov@tu-sofia.bg (H.U.)
* Correspondence: sdechkova@tu-sofia.bg; Tel.: +359-8-9702-2422

Abstract: In most cases, the dynamic investigation of vehicle collisions with stationary obstacles concerns solutions to complex tasks related to the identification of occupant position in the vehicle. The motion of the bodies in the car is determined by the intensity of the inertial coordinate system, also known as moving reference frame, invariably fixed to the vehicle's center of mass. The focus of the study is on how forces of inertia change their magnitude and direction in the car's motion. This requires specific analysis carried out by dividing the vehicle trajectory into separate stages according to certain indicators, such as free motion, impact process, and post-impact residual motion. Particular attention has been paid to the impact itself, in which the forces of inertia are the most intense, and their magnitude and direction change abruptly. A solution to a Cauchy problem has been found, in which initial kinematic parameters of the crash process are considered, satisfying the kinematic values at rest position.

Keywords: inertial forces; impact; passengers; finite element method; Abaqus

check for updates

Citation: Karapetkov, S.; Uzunov, H.; Dechkova, S.; Uzunov, V. Impact of Inertial Forces on Car Occupants in a Vehicle-Fixed Barrier Front Crash. *Symmetry* **2023**, *15*, 1998. https://doi.org/10.3390/sym15111998

Academic Editors: Guangdong Tian, Chong Wang, Vladimir A. Stephanovich and Sergei D. Odintsov

Received: 11 May 2023
Revised: 27 September 2023
Accepted: 25 October 2023
Published: 30 October 2023

1. Introduction

Investigating car occupant behavior in a traffic collision implies finding a solution to a mixing problem with differential equations. Therefore, identifying separate motion phases seems to be of the utmost significance. The first phase is prior to impact, the second one is the impact itself, and the third one is the post-impact motion. The present dynamic investigation is based on the identification of occupant position in relation to the vehicle's symmetrically located axes and the effect of seat belts in each separate motion phase. The findings showed that inertial forces magnitude in separate motion phases was variable and the time for its change could be determined and estimated. Thus, the possibility of applying passive safety systems enhances so as to prevent vehicle occupant injuries and to reduce the risk of death.

The motion of a body in the car is determined according to the inertial forces' intensity in the translation coordinate system, also known as moving reference frame, invariably attached to the vehicle's center of mass [1–6]. In each phase of the vehicle's motion, the inertial forces change magnitude and direction, due to the change in magnitude of the absolute value of acceleration and angular velocity. The components of inertial forces at each place in the car, in the separate motion phases, have various magnitudes and directions, which determine the different impacts of the safety belt. The analysis carried out is based on occupant position in relation to the vehicle's symmetrically located coordinate system. The mixing problem refers to the dynamic investigation of each separate motion phase and the determination of the net force magnitude, the vector sum of all inertial forces. Subsequently, what is required for a detailed analysis is dividing the vehicle's motion trajectory into separate stages according to the following indicators: free motion, impact process, and post-impact vehicle motion based on residual kinetic energy. Pre-impact motion has been analyzed by taking into consideration the driver's steering behavior, frictional forces' impact, and the exertion of inertial forces on vehicle occupants arisen due

to previous two parameters. In the impact phase, a Cauchy problem was investigated using the finite element method for the dynamic study. The final magnitude of the velocities of vehicle's center of mass and angular velocity were initial values of the differential equations of motion after the impact, satisfying the final position of the car at rest defined in a fixed coordinate system.

2. Dynamic Model of a Vehicle-Fixed Barrier Front Crash

In the present paper, an analysis of the car's motion in three separate phases is presented by solving a mixing problem with differential equations. The first phase of motion refers to a dynamic study of driver behavior when specific actions have been taken to turn the steering wheel and a loss of control has occurred. Consequently, the vehicle has left the traffic lane and hit a roadside tree. The tree impact phase investigates dynamically changing quantities, and the residual kinetic energy determines the car's motion in the third and last phase.

The aim of the present paper is to design and come up with a dynamic model of a vehicle-fixed barrier front crash in three separate motion phases and to investigate the inertial forces' impact on occupant behavior in the passenger compartment. While predicting dynamically changing values and inertial forces, the impact of passive safety systems has been also determined [7–12].

Under the action of inertial forces, there is a relative displacement of the bodies inside the occupant compartment, and the amount of displacement depends on whether they are wearing safety belts or not. If a deep and close look is to be taken when solving the mixing problem, rear weight transfer time and translation inertial force generation could be predicted. Translation inertial force direction depends on the direction of acceleration, while its magnitude refers to the passenger's body mass and the magnitude of acceleration.

According to D'Alembert's principle, the first main force acting on bodies and considered in the vehicle translation coordinate system is the fictitious translation force. It is determined using the following expression:

$$\vec{F}_e = -m \cdot \vec{a}_e = -m \cdot \left[\vec{a}_c + \vec{\varepsilon} \times \vec{\rho} + \vec{\omega} \times \vec{\omega} \times \vec{\rho} \right] \quad (1)$$

where m is the mass of the passenger; $\vec{a}_e$ is the fictitious translation acceleration; $\vec{a}_c$ is the acceleration of vehicle's center of mass; $\vec{a}_{cc}$ is the Coriolis acceleration of the body center of mass; $\vec{\omega}$ is the angular velocity of the vehicle; $\vec{\varepsilon}$ is the vehicle angular acceleration; and $\vec{\rho}$ is the radius vector of the body center of mass relative to the vehicle's center of mass.

The car's motion in the separate motion phases is also related to the angular velocity vector, and the one around the vertical axis is mainly considered here, i.e., the vehicle's motion in the plane of the road and the rotation around the vertical axis when the loss of control occurs. Under the action of angular velocity vector and the displacement of the passenger's body in the occupant compartment, another main inertial force is generated, namely Coriolis translation inertial force. It is of the following type:

$$\vec{F}_c = -m \cdot \vec{a}_{cc} = -2 \cdot m \cdot \left[\vec{\omega} \times \vec{V}_r \right] \quad (2)$$

where $\vec{V}_r$ is the relative velocity of the body center of mass in relation to the vehicle moving reference frame.

In the car's motion phases and the subsequent rotation with the variable angular velocity vector, a variable magnitude of centrifugal inertial force arises. The magnitude of the inertial force generally depends on the three-component direction of the vector $\vec{\omega}$, which is the angular velocity vector. Due to the small magnitude of the angular velocity

vector around its longitudinal and transversal axis, the investigation has been carried out without a vehicle rollover but rotating around the vertical axis passing through the center of mass of the car coordinate system, symmetrically located with respect to the car body. The magnitude of the centrifugal inertial force has the following form:

$$\vec{F}_{e\omega} = m \cdot \omega^2 \cdot \vec{\rho} \tag{3}$$

where $\vec{\rho}$ is the distance from the body center of mass to the vehicle's center of mass. This distance is variable and depends on the distance of the body's center of mass to the vehicle's center of mass in the movable coordinate system.

In the car's motion in its separate phases of deceleration caused by the action of frictional forces and in the phase of loss of lateral resistance, the main effect on occupant bodies comes from the translation inertial force caused by the deceleration of retarded motion. It has the following form:

$$\vec{F}_{ec} = -m \cdot \vec{J}_e \tag{4}$$

$\vec{J}_e$—translation acceleration in retarded motion.

Initial conditions for solving a mixing problem with differential equations, also called a Cauchy problem, are the initial conditions at each stage, obtained as final conditions of the previous one. In addition, in each motion phase, there are preset coordinates from tire tracks obtained from the motion of the wheels on the ground. They are fixed in a preselected fixed coordinate system. Furthermore, the coordinates of the final position of the car's center of mass at rest and the angle of rotation of the moving coordinate system invariably attached to it, relative to the translationally moving one and connected to its center of mass, are known.

To carry out the dynamic investigation, a case study of a road accident with a Mercedes is presented where the driver loses control, leaves the road and hits a roadside tree. As a result of the impact and due to the inertial forces exerted on the passengers, one of them is propelled from the car and hurled into the air. In this particular event of traffic accident, the passenger reaches a state of final position at rest outside the car.

The characteristics and main signs of road accidents of such a type are the typical deformations from the contact of the car with the roadside tree relative to the symmetrically located car coordinate system. In the first phase of motion, the car has moved with relative transverse friction between the tires and the road surface, and the motion trajectory is arc-shaped. The car has crossed the entire traffic lane diagonally and what follows is an impact into the roadside tree (Figures 1 and 2) [13–16].

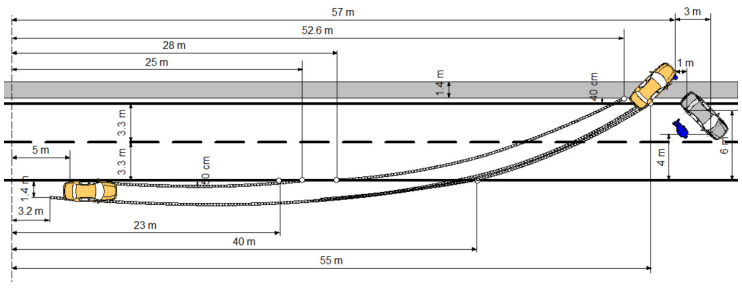

Figure 1. Accident reconstruction's drawing and sketch.

Figure 2. Post-impact position of vehicle and passengers involved in the car accident.

As long as the kinematic quantities in the motion phases are known, it would be possible to sufficiently predict the magnitudes and directions of each component of the inertial forces, including the magnitude of the resultant vector sum. Obtaining the total magnitude of the vector sum of the inertial forces acting on a given body in the car compartment also determines the passive safety systems' impact. The analysis takes into consideration and compares known and established parameters, such as the coordinates of the points of the centers of the wheels with tire tracks on the road, the coordinates of the center of mass with final position of the vehicle at rest, and the coordinates of the final position of the passenger body at rest with received body injury characteristics. The presence of a complete coincidence of such indicators and circumstances determines the reliability of the applied dynamic model and the assessment of the effect of the technical means for passive safety.

As a result of the impact with the tree, the car has been deformed in an area relative to its coordinate system, which is symmetrically located with respect to the car body. This deformation is mainly in the area of the engine compartment and with a main direction from right to left and from front to back, viewed from the rear of the car. Upon contact with the tree, characteristic deformations have been made, the shape of which resembles that of the base of the tree stem. The deformation area thus defined is typical for such contact of the body with the roadside tree and the penetration that occurred during that specific motion phase. Another aspect of the investigation is the deformation of different type and direction and in the area of the front right door. There is a bulging of the surface from the inside out relative to the car's coordinate system, invariably related to its center of mass (Figure 3). The direction of deformation of this car body element does not correspond to the direction of deformation from the contact with the tree. This means that the nature and intensity of the deformation is a sign of the action of other forces generated by another body, thus being the exertion of inertial forces. Logical questions in the research are how the inertial forces have affected the position of the occupant bodies in the car in the separate phases and who or what has caused the damage to the element of the car's body. Another question is how would seat belts affect the vehicle occupant safety.

Figure 3. Deformations on the automobile.

The answer to this question can be obtained by studying the macro motion of the car in three separate phases—the phase of loss of transverse stability prior the impact, the impact phase, and the phase of post-impact vehicle motion.

Technical data for the Mercedes-Benz E-Class (W124): length 4740 mm; width 1740 mm; height 1430 mm; wheelbase 2800 mm; front trace 1501 mm; rear trace 1491 mm; and gross vehicle weight 1520 kg. Moment of inertia about the vertical axis $J_z = 2460$ kg·m^2.

The coordinates of the vehicle's center of mass at the time of initial contact before the deformation phase and the angle of rotation about the vertical axis of the vehicle, relative to the selected fixed coordinate system, are as follows:

$$x_c = 55.1 \text{ m};\ x_c = 4.9 \text{ m};\ \varphi_z = 45^\circ \tag{5}$$

The velocity of the center of mass at the moment of impact relative to the mobile coordinate system invariably fixed to the vehicle is as follows:

$$V_{x'} = 51.5 \text{ km/h};\ V_{y'} = 39.7 \text{ km/h} \tag{6}$$

3. Results of the Dynamic Study

The impact phase is considered by solving a Cauchy problem, where a solution is found regarding the depth of deformation in the right-side front part, as well as the data on the initial conditions of the kinematic quantities satisfying the final position of the car at rest in micro motion after the impact (Figure 4). Figure 5 shows the impact deformation between a car and a tree via the finite element method using the Abaqus 2022/Explicit software product [17–22].

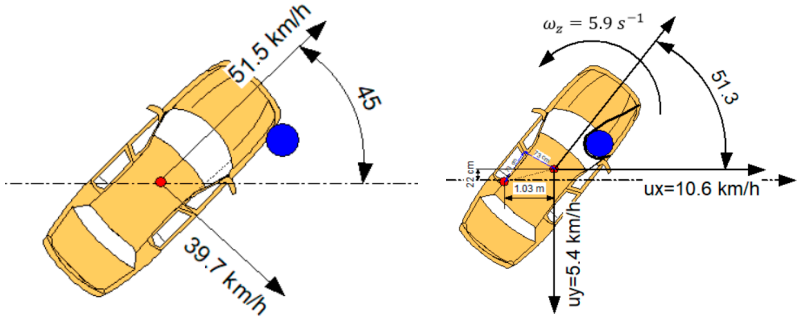

(**a**) Initial location of collision point (**b**) Post-impact location

Figure 4. Data on the position of the car at initial contact and final position in the deformation phase. (**a**) Initial location of collision point. (**b**) Post-impact location.

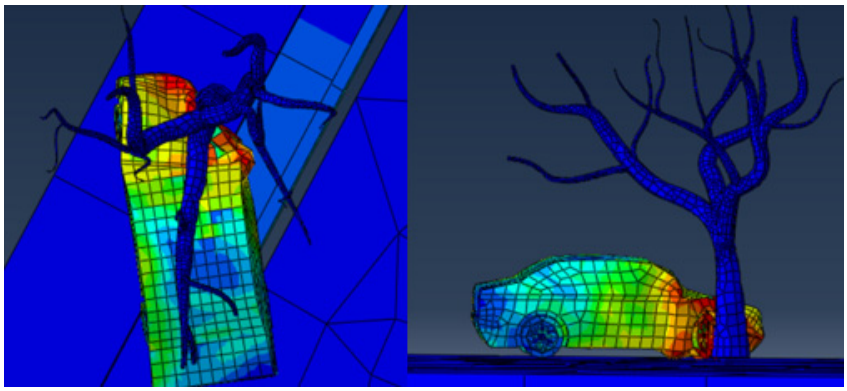

Figure 5. Deformation resulting from an impact between a car and a tree obtained using the Abaqus/Explicit software product.

The car crashing into the tree is characterized by the impulse–momentum theorem for the time of impact, which has the following form:

$$m \cdot \vec{u} - m \cdot \vec{V} = \vec{S} \tag{7}$$

Here, $\vec{u}$ is the post-impact velocity of the car's center of mass; $\vec{V}$ is the prior-to-impact velocity of the car's center of mass; and $\vec{S}$ is the crash pulse.

According to the theorem, the velocity of the car's center of mass varies in direction, magnitude and position, and its change is determined using the following expression (Figure 6):

$$\vec{u} - \vec{V} = \Delta\vec{V} \tag{8}$$

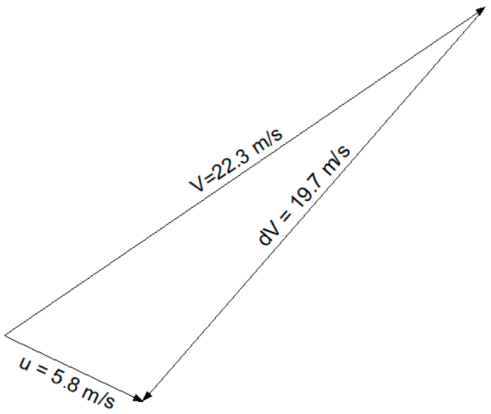

Figure 6. Velocity vector car map.

The impulse–momentum change theorem with respect to the car's center of mass, applied in the impact theory, takes the following form:

$$I_c(\omega - \omega_o) = S \cdot d \tag{9}$$

where I_c is the vehicle moment of inertia relative to its vertical central axis; ω is the post-impact angular velocity; ω_o is the pre-impact angular velocity, negligibly smaller compared to the post-impact angular velocity; S is crash pulse; and d is the slope of the crash pulse.

The right side of the equation represents the moment of the crash pulse relative to the car's center of mass. The impact on the car is accompanied by a significant deformation in the lateral front right part as the impact force is in front–back and right–left direction relative to the vehicle's own coordinate system.

After crashing into the tree, the car spins strongly, acquiring a significant angular velocity in a counterclockwise direction as viewed from above. In order to have a match between the traces and the trajectory of the car's motion after the impact, the crash pulse must pass from the left side of the car's center of mass as seen from above, creating a momentum relative to the center of mass, thus causing a kinetic momentum and the described rotation, respectively. The velocity of the car's center of mass before the impact is determined via Delta-V [15,23]. A point to consider in this study is that the angular velocity around the vertical axis in the impact phase is not taken into account. In addition, the velocity of the car's center of mass after the impact is obtained in accordance with the theorem of the motion of the center of mass while crashing into the tree until its final position at rest.

$$m \cdot \frac{\vec{du}}{dt} = \sum \vec{F}_i \tag{10}$$

where m is the mass; u is the velocity of the center of mass of the given car after the impact; $\sum \vec{F}_i$ is the acting resistance forces.

After separating the variables and integrating, for the time interval from initial rotation to impact, we obtain the following:

$$m \cdot \int_0^1 u \cdot du = \int_0^1 \sum F_{i\tau} \cdot ds \tag{11}$$

where the friction force is $F_\tau = -\mu \cdot m \cdot g$. Here, $\mu = 0.8$. μ^* is the coefficient of transverse friction between the tires and the road surface; and $g = 9.81$ m/s^2 is the Earth's acceleration.

After integration according to the initial conditions, we ibtain the post-impact velocity of the car's center of mass, as follows:

$$u = \sqrt{2 \cdot \mu_1 \cdot s_1 \cdot g} \tag{12}$$

where $s_1 = 4.9$ m is the distance for the car's center of mass after crashing into the tree, respectively, and g is the acceleration gravity.

We obtain the following:

$$u = \sqrt{2 \cdot \mu_1 \cdot s_1 \cdot g} = \sqrt{2 \cdot 0.35 \cdot 4.9 \cdot 9.81} = 5.8 \text{ m/s} = 20.9 \text{ km/h} \tag{13}$$

The given coefficients characterizing the elasticity and strength of the structure of the class of cars for the type Mercedes 200 D (longitudinal base 2.82 m)—stiffness coefficients upon impact, respectively, in [N/cm] and [N/cm^2]—for side impact are as follows:

$$\begin{array}{c} A = 240 \ \frac{\text{N}}{\text{cm}}; \\ B = 65.5 \text{ N/cm}^2 \end{array} \tag{14}$$

Energy loss due to impact is determined using the following formula:

$$E = (1 + \text{tg}^2\alpha)\frac{L}{5}\begin{bmatrix} \frac{A}{2}(c_1 + 2c_2 + 2c_3 + 2c_4 + 2c_5 + c_6) \\ +\frac{B}{6}(c_1^2 + 2c_2^2 + 2c_3^2 + 2c_4^2 + 2c_5^2 + c_6^2 \\ +c_1c_2 + c_2c_3 + c_3c_4 + c_4c_5 + c_5c_6) + 5\frac{A^2}{2B} \end{bmatrix} \tag{15}$$

where $\alpha = 65^\circ$ is the angle between the normal of the impact surface and the crash pulse; $L = 1.0$ m is the width of deformation in [m]; $c_i/i = 1, 2 \ldots 6/$ is the size of the deformation in six points, evenly distributed across the width, in [cm] $c_1 = 0$ cm; $c_2 = 25$ cm; $c_3 = 48$ cm; $c_4 = 52$ cm; $c_5 = 45$ cm; $c_6 = 35$ cm. The data from the analysis are summarized in Tables 1 and 2 below.

Table 1. Delta-V method when a car hits a stationary object.

Delta-V Method When a Car Hits a Stationary Object	
Total mass of the vehicle	1500.00
Depth of deformation at first point c_1 in [cm]	0.00
Depth of deformation at second point c_2 in [cm]	22.00
Depth of deformation at third point c_3 in [cm]	44.00
Depth of deformation at fourth point c_4 in [cm]	48.00
Depth of deformation at fifth point c_5 in [cm]	40.00
Depth of deformation at sixth point c_6 in [cm]	31.00
Angle between the surface normal and the impact force in degrees	65.00
Deformation width in [m]	1.00
Angle of velocity direction of center of mass before impact in degrees of X	31.00
Angle of velocity direction of center of mass after impact in degrees of X	334.00
Crash coefficient A in [N/cm]	240.00
Crash coefficient B in [N/cm^2]	65.50
Distance travelled from the center of mass after the impact in the first section in [m]	4.90
Reduced coefficient of friction in the first section	0.35

Table 2. Vehicle speed data.

Vehicle Speed Data	$[u_{ij}; V_{ij}]$	
Post impact speed of vehicle [m/s]	5.80	[m/s]
Post impact speed of vehicle [km/h]	20.88	[km/h]
Velocity change for the vehicle dV [m/s]	19.66	[m/s]
Velocity change for the vehicle dV [km/h]	70.78	[km/h]
Pre-impact speed of vehicle [m/s]	22.19	[m/s]
Pre-impact speed of vehicle [km/h]	79.90	[km/h]
Angle between the velocity vector before and after impact	303.00	[o]
Strain energy E	289,938.87	[N·m]

The velocity of the car's center of mass at the moment of impact is calculated using the following formula:

$$V_y = \sqrt{\left|\vec{\Delta V}\right|^2 - \sin^2 \gamma \cdot u^2} + \cos \gamma \cdot u \tag{16}$$

where $\gamma = 58^{\circ}$ is the angle between the velocities of the car's center of mass prior to and post impact.

The dynamic analysis thus defined has some inaccuracy due to the fact that the angular velocity of the car's motion in the impact phase has not been taken into account as well as in the second and third phases. Moreover, the dynamic component of the centrifugal inertial force and the Coriolis inertial force, which also require the magnitude of the angular velocity around the vertical axis, could not be determined using the method applied.

The implementation of the finite element method allows for a detailed analysis of the inertial forces acting on the bodies to a significantly greater extent.

Detailed finite element modeling enables the development of a vehicle collision with a tree in the Abaqus/Explicit environment (Figure 7). In the model, the elements are separated into two levels—primary and secondary—which allows for meshing with lower density, compared to the usual one-level approach. The second-order tetrahedral element has 10 nodes (4 corner nodes and 6 internal nodes), each with three degrees-of-freedom. After the deformation, the edges and surfaces of the secondary elements are converted into curved shapes. Thus, the application of the chosen method, the curvilinear shapes, suggests an advantage over that of others and is justified.

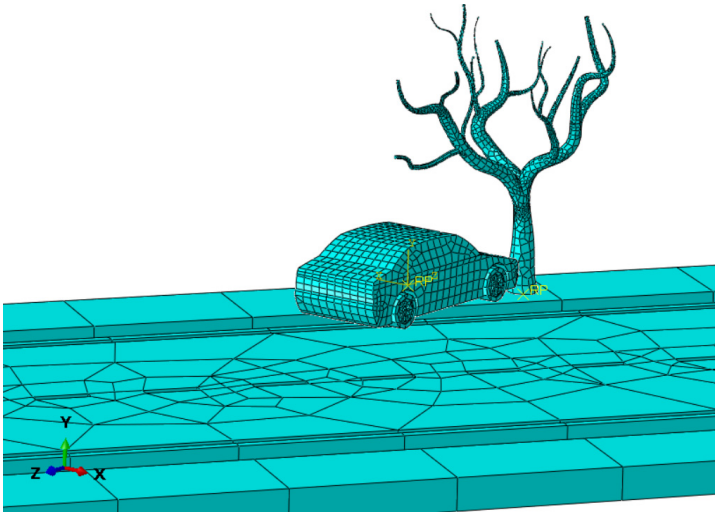

Figure 7. Finite element model of car and tree in Abaqus.

The use of tetrahedral finite elements is an advantage in the synthesis of second-order displacement fields and is applicable to a variety of analyses in Abaqus/Explicit.

The degrees of freedom of a node in a finite element network determine its translational capability. The number of degrees of freedom in a node depends on the type of element to which it belongs.

Using Abaqus/Explicit in a critical stage of the analysis, such as meshing, is advantageous because the generated mesh is associative, depending on the element dimensions.

When selecting a material in Abaqus/Explicit, it is assumed that stress is linearly related to strain. The selected isotropic steel Steel-30XGSA is suitable because it has a plastic zone characterized by large deformations accompanied by small changes in stresses. The yield strength of the created object is 355 MPa and hardens to a final value of 490 MPa, at a plastic strain of 0.025. When creating the model for the vehicles and pedestrians, the principles of solid modeling are generally applied. This is carried out to avoid inaccuracies in obtaining the output results. The objects are modeled with standard shell elements (Abaqus elements S3R and S4R) with a thickness of 0.01 m. Loads are applied step by step. In the presence of nonlinearities, each load step consists of several iterations. This also implies the possibility of its own type of boundary conditions and output data analysis for each load step. In the present case, a step of 21 iterations is set.

Defining the boundary conditions in the analysis is related to bonding certain surfaces of the created model. Loads are represented using gravity force distributed over volume and accounting for self-weight. With this type of loading, Abaqus calculates the magnitude of the gravitational force for each individual element, taking into account the density of the material.

Figures 8 and 9 show projection variations in velocity center of mass and angular velocity with respect to the vertical axis in the impact phase. For the impact time of 0.025 s, the values of the projections of the velocities, the angular velocity around the vertical axis, as well as the coordinates of the center of mass with the rotation angle towards the final phase of the impact, are as follows:

$$\begin{gathered} u_{xc} = 4.85 \text{ m/s}; u_{yc} = -2.6 \text{ m/s}; \omega_z = 5.9 \text{ s}^{-1} \\ x_c = 3.33 \text{ m}; \; y_c = 4.42 \text{ m}; \; \varphi_z = 51.3^\circ \end{gathered} \tag{17}$$

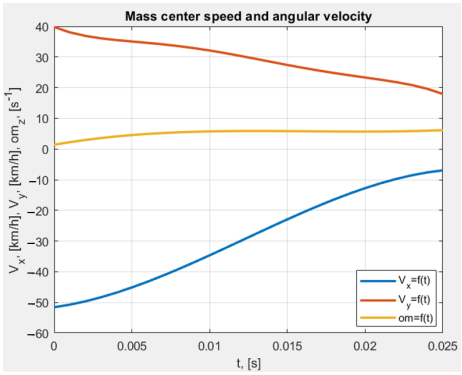

Figure 8. Change in the projections of the velocity of the center of mass and the angular velocity about the vertical axis at impact stage.

The kinematic quantities represent the initial values of the differential equations of motion in the last stage of the car macro motion after the impact, respectively, until the final position at rest. To demonstrate the high reliability of the study, the coordinates of the center of mass and the angle of rotation about a vertical axis in the final position at rest has been compared to the actual one. If the solutions do not satisfy, multiple iterations are performed until a complete match.

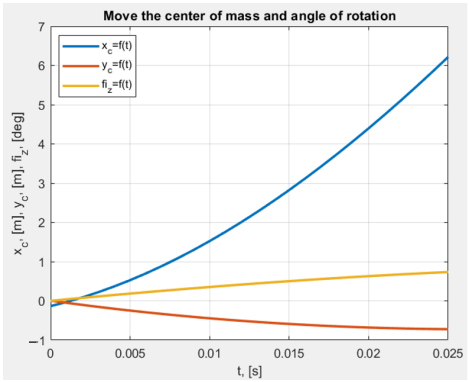

Figure 9. Change in the coordinates of the center of mass and angle of rotation about the vertical axis at impact phase.

The stationary coordinate system $OXYZ$ is assumed to have an arbitrary origin relative to which the macromotion of the car is investigated. Two more coordinate systems are introduced for the dynamic study. The first one starts at point C, denoted as $Cx'y'z'$, invariably connected to the car, parallel to the absolute coordinate system $OXYZ$, and is displaced linearly and parallel to the absolute coordinate system. The second coordinate system has the same origin, respectively, point C, and is designated $Cxyz$; it is mobile and rotated at the angles ψ, θ and φ (Figure 10) relative to the translationally moving $Cx'y'z'$.

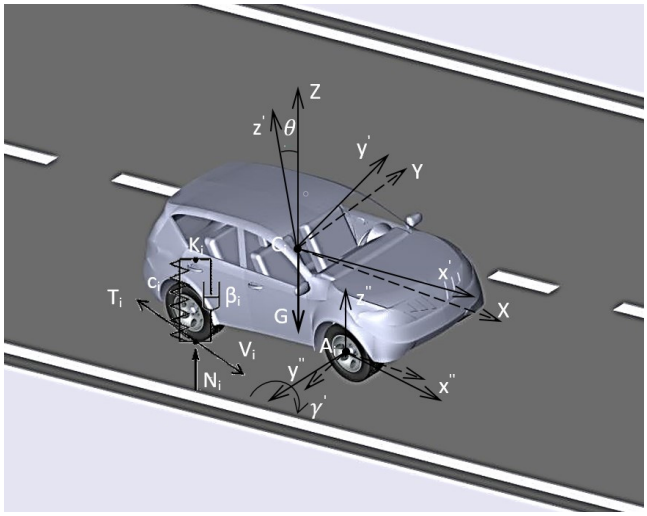

Figure 10. Spatial dynamic model of an automobile with elastic suspension.

The coordinates of the center of mass C of the vehicle x_c, y_c, z_c in the stationary coordinate system are selected as generalized coordinates of the vehicle's motion.

Euler transformations with angles ψ, θ and φ represent the rotational motion of the car. ψ is the precession angle, taking into account the rotation around the Cz axis. Angle θ is the nutation angle, accounting for the rotation relative to the axis C_ρ, the intersection of the planes O_{xy} and $C_{x'y}$.

The gravity force $\vec{G}$ is assumed to lie on the Oz axis. The dynamic research model is a plane located in space, which is on four elastic supports, denoted by $K_i (i = 1 \div 4)$ (Figure 11).

$\vec{F}_i (i = 1 \div 4)$ elastic strength, taking into account the total elastic constant of tires and springs;

$\vec{N}_i (i = 1 \div 4)$ a normal reaction at the contact point of automobile tires according to Coulomb's law and its relation to the friction force;
$\vec{V}_i (i = 1 \div 4)$ the velocity vector of the contact point P_i which lies on the plane along path Oxy;
$\vec{T}_i (i = 1 \div 4)$ frictional force with the directrix passing through the point of contact, the vector of which lies in the plane along path Oxy;
$\vec{R}_i (i = 1 \div 4)$ resistance force generated by the damping elements in the suspension;
c_i, $\frac{N}{m} (i = 1 \div 4)$ coefficient of elasticity of each wheel suspension, a total value of the tires and springs;
b_i, $\frac{N \cdot s}{m} (i = 1 \div 4)$ coefficient of linear resistance, taking into account the degree of damping oscillations in the elastic elements of the suspension.

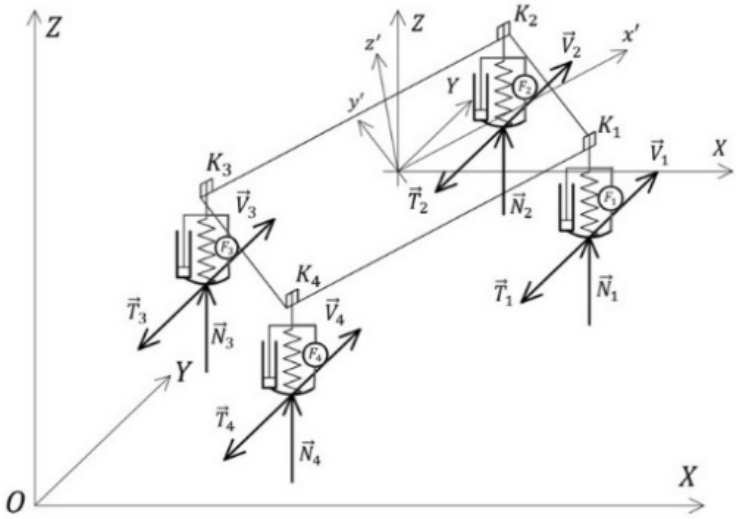

Figure 11. Model of the forces acting on a car in its spatial motion, taking into account the elasticity of tires (suspension).

Six differential equations with six generalized coordinates are defined, respectively, for three linear displacements and three rotations during the car's motion, obtained according to the Lagrange second-order equations, analyzing the kinetic energy and generalized forces.

Assuming that the absolute coordinate system has a vertical axis Oz, we determine the generalized forces and moments that are on the right-hand side of the differential Equations (18) and (19).

Linear displacement of the car's center of mass is determined using the three generalized coordinates relative to a selected Cartesian coordinate system.

$$[B_{ij}] \cdot \begin{bmatrix} \ddot{x} \\ \ddot{y} \\ \ddot{z} \end{bmatrix} = [F]$$
$$[F] = \begin{bmatrix} \sum_{i=1}^{4} F_{xi} \\ \sum_{i=1}^{4} F_{yi} \\ -G + \sum_{i=1}^{4} N_i - \sum_{i=1}^{4} R_i \end{bmatrix} \quad (18)$$

where $[B_{ij}]$ is a square matrix of the mass parameters of the car; $\begin{bmatrix} \ddot{x} \\ \ddot{y} \\ \ddot{z} \end{bmatrix}$ is a column matrix of the accelerations of the center of mass; and $[F]$ is the matrix pillar from the projection of external active forces.

The rotation of the car is determined viz the three Euler angles, and the angular accelerations obtained from them.

$$[A_{ij}] \cdot \begin{bmatrix} \ddot{\varphi} \\ \ddot{\psi} \\ \ddot{\theta} \end{bmatrix} = [M_{ij}]$$

$$[M_{ij}] = \begin{bmatrix} \sum_{i=1}^{4} M_{Ni} + \sum_{i=1}^{4} M_{Ri} + \sum_{i=1}^{4} M_{Fi} + \left(\sum -b_i \cdot \dot{q}_i^2\right) + \left(\sum -c_i \cdot \dot{q}_i \cdot \dot{q}_j\right) \\ \sum_{i=1}^{4} M_{Ni} + \sum_{i=1}^{4} M_{Ri} + \sum_{i=1}^{4} M_{Fi} + \left(\sum -b_j \cdot \dot{q}_j^2\right) + \left(\sum -c_j \cdot \dot{q}_j \cdot \dot{q}_k\right) \\ \sum_{i=1}^{4} M_{Ni} + \sum_{i=1}^{4} M_{Ri} + \sum_{i=1}^{4} M_{Fi} + \left(\sum -b_k \cdot \dot{q}_k^2\right) + \left(\sum -c_k \cdot \dot{q}_i \cdot \dot{q}_k\right) \end{bmatrix} \quad (19)$$

where $[A_{ij}]$ is a square matrix of the coefficients in front of the accelerations as a function of the moments of inertia; $\begin{bmatrix} \ddot{\varphi} \\ \ddot{\psi} \\ \ddot{\theta} \end{bmatrix}$ is a column matrix of the angular accelerations obtained from the selected generalized coordinates, namely Euler angles; $[M_{ij}]$ is a column matrix of the sum of the moments of normal reactions in the wheels, the moments of damping forces, the moments of frictional forces, the moments of inertial forces; and $\dot{q}$ is the angular velocity for each generalized coordinate.

Four more differential equations are introduced according to the kinetic energy momentum theorem concerning the wheels' relative motion. They are of the following type:

$$[I_\gamma] \cdot [\ddot{\gamma}] = [M_{\gamma i}];\ M_{\gamma i} = \left\{F_{i\tau} \cdot r_i + sign\ (\dot{\gamma}_i) \cdot [M_{di} - f_i \cdot N_i - M_{si}]\right\} \quad (20)$$

The analysis of the equations in the motion of the wheels takes into consideration the tangential friction force $\vec{F}_{i\tau}$. This force is located in the plane of the road. Its direction is opposite to the direction of the velocity of the contact point. It changes its direction during velocity vector analysis.

The assumed coefficient of friction $\mu(V_P)$ is considered to be variable and dependent on the speed of the contact point; the kinematic radius of the wheel $\vec{r}_i$ is taken into account; the analysis also uses a coefficient of friction caused by the rolling of the car wheel, indicated as f_i; the contact of each wheel with the road surface is determined via the normal reaction $\vec{N}_i$; and $[I_\gamma]$ represents the mass moments of inertia for each wheel form a square matrix and are the coefficients in front of the angular accelerations $\dot{\gamma}_i / i = 14/$. After integrating the angular accelerations, the angular velocity of each wheel is obtained; $[\ddot{\gamma}]$ represents the angular accelerations of each wheel form a column matrix, taking into account whether the vehicle has two drive wheels or four; M_{di}, M_{si}. The research was also carried out taking into account the corresponding values of the engine moment when it is reduced to each drive wheel and the corresponding braking moment in case of activation of the brake system.

Figure 12 shows a diagram of an active car suspension. Figure 13 shows a diagram of a drive wheel.

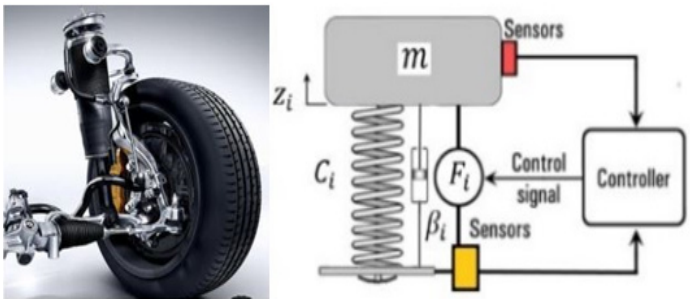

Figure 12. Dynamic model of an active suspension system.

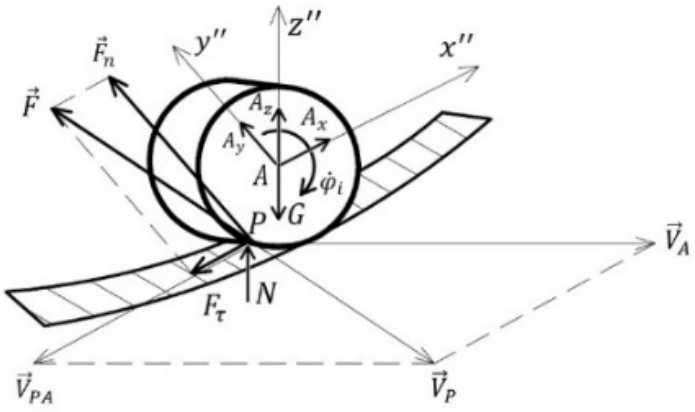

Figure 13. Drive wheel diagram.

The solutions of the system of differential equations of motion (8) and (9) are shown graphically (Figures 14–17).

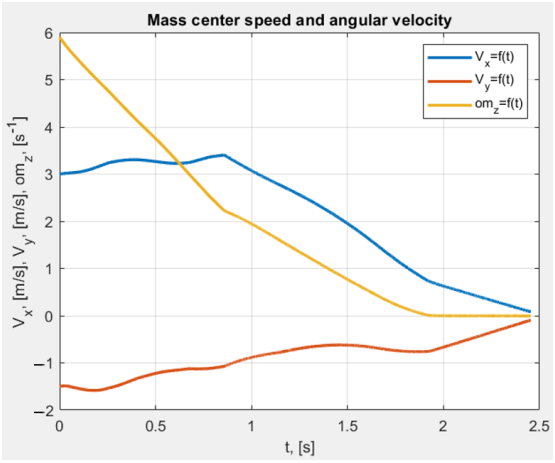

Figure 14. Change in the projections of velocity center of mass and angular velocity.

The dynamic study of the car's motion in the impact phase has found out that inertial force from retarded motion has the smallest component and it does not significantly affect the occupant's motion in the car compartment. The dominant forces at impact for each of the bodies are translation inertial forces resulting from the significant change in the velocity of the center of mass in a short time interval, which is about 0.025 s. The bodies move along the direction of the velocity vector given enormously larger translation accelerations at impact. After the impact and the car's subsequent motion, the main inertial forces are, respectively, centrifugal inertial force and inertial force from retarded motion, the latter being negligibly small compared to the centrifugal one (Figure 18).

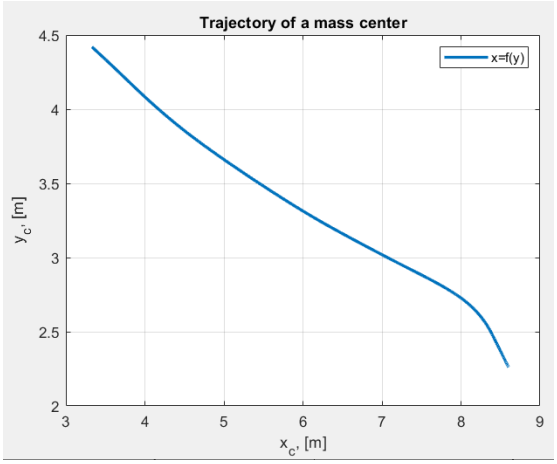

Figure 15. Trajectory of the vehicle's center of mass after the impact.

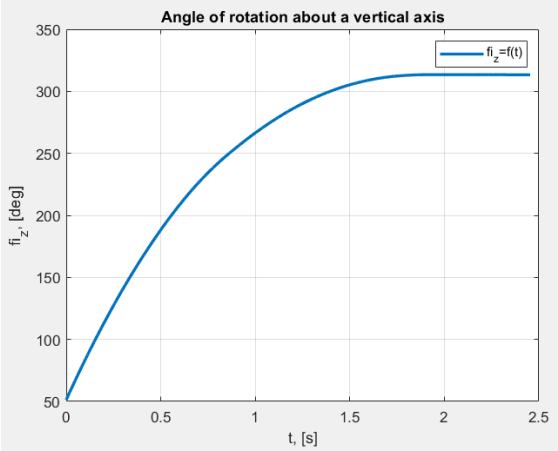

Figure 16. Change in rotation angle about a vertical axis after impact.

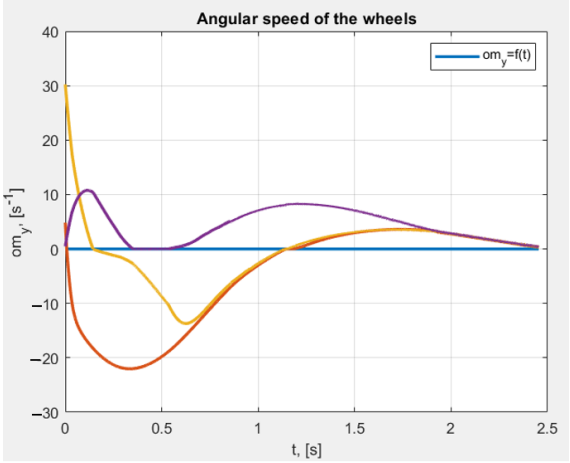

Figure 17. Change in wheels angular velocity after impact.

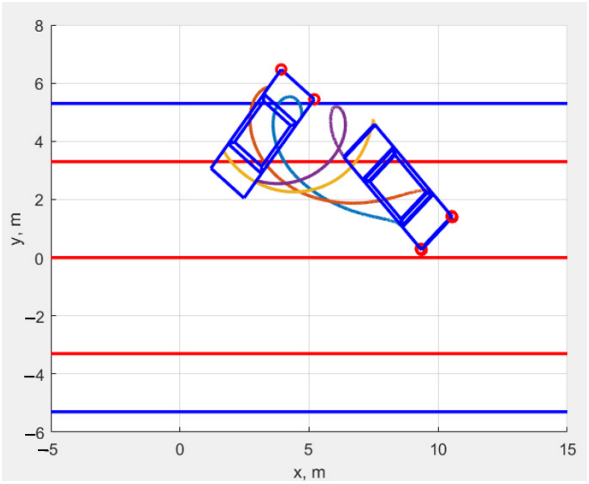

Figure 18. Discrete positions of vehicle's motion.

During impact, the main and dominant force is the translation inertial force and it is due to the acceleration of the center of mass in the deformation phase of the car. The car's motion is mainly translational, without appreciable rotation (Figure 19). The translation inertial force has the following form:

$$\vec{F}_{ec} = -m \cdot \vec{a}_{cy1} = -\frac{m}{\tau} \cdot d\vec{V} \tag{21}$$

where τ is the time of impact; $\vec{a}_{cy1}$ is the acceleration of the center of mass during impact; $d\vec{V}$ is the change in the speed of the car's center of mass. This force component occurs first at impact and sharply decreases afterwards when maximum deformation is made. After impact, it ceases to act, and the dominant ones are the centrifugal force and the force from retarded motion.

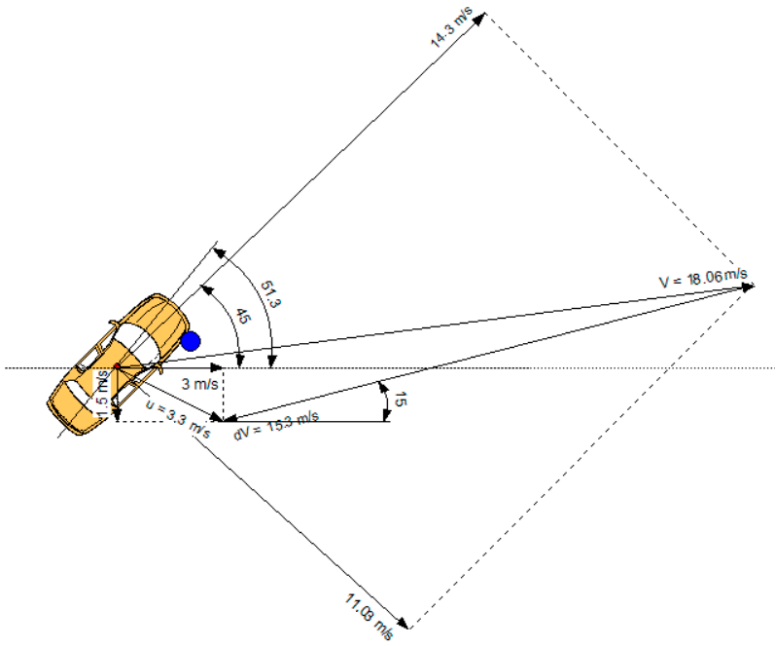

Figure 19. Vector plan of change in the velocity of the center of mass at impact.

The impact is specified by the impulse–momentum change theorem/impulse–momentum theorem for the time of the impact, which has the following form:

$$m \cdot \vec{u} - m \cdot \vec{V} = \vec{S} \tag{22}$$

Here, $\vec{u}$ is the velocity of the vehicle's center of mass after the impact; $\vec{V}$ is the vehicle velocity of the center of mass immediately before the impact; and $\vec{S}$ is the vehicle crash pulse.

According to the theorem, the vehicle velocity of the center of mass varies in position, magnitude and direction, and its change is determined via the following expression:

$$\vec{u} - \vec{V} = \Delta\vec{V} \tag{23}$$

Taking into account the magnitude of velocity change, this force for the driver and passenger bodies takes, for example, the following form:

$$\left|\vec{F}_{ec}\right| = \left|-\frac{m_p}{\tau} \cdot dV\right| = \frac{80}{0.025} \cdot 15.3 = 48960 \text{ N} \tag{24}$$

Under the action of this very large force, the bodies tend to move forward and slightly to the right at an angle of about 15° to the longitudinal axis of the vehicle. This direction was obtained as a result of the performed dynamic study of the vector of the change in the velocity of the center of mass in the impact phase. The body's motion under the action of this force is significant in case of not wearing a seat belt. The essential moment in the study is that this direction of acceleration of the translation inertial force is in complete accordance with safety belt functions. In modern cars, the speed of the gas generators has increased significantly, and the resulting impact time is within the safe range. In this particular case, the passenger's body in the front right seat has moved forward and to the right, deforming the front right door. It is obvious that for such deformation and body motion to occur, the occupant was not wearing a seat belt.

The analysis takes into consideration another major problem that arises at such massive impacts, namely the acceleration that the internal organs receive under the effect of wearing the seat belt. In most cases, the belt prevents the possibility of changing the body position, but there is significant internal organ damage, like internal bleeding or organ failure.

Next, another major component is the translation inertial force due to post-impact angular velocity of the car or the so-called centrifugal translation inertial force. Its magnitude is determined via the following formula:

$$F_{e\omega} = m_p \cdot \rho \cdot \omega_z^2 \tag{25}$$

where ρ is the distance from the body's center of mass to the vehicle's center of mass at the moment of impact. This distance consequently changes with the movement of the bodies in the car. Its size at the initial moment of rotation is as follows:

$$F_{e\omega} = 80 \cdot 1 \cdot 5.9^2 = 2785 \text{ N} \tag{26}$$

The variation in the centrifugal inertial force is as shown in Figure 20.

It is apparent that the magnitude of angular velocity at the initial moment is the largest. This definitely affects the position of the body, as in the specific case, under the action of this inertial force, the body has been propelled from the passenger compartment.

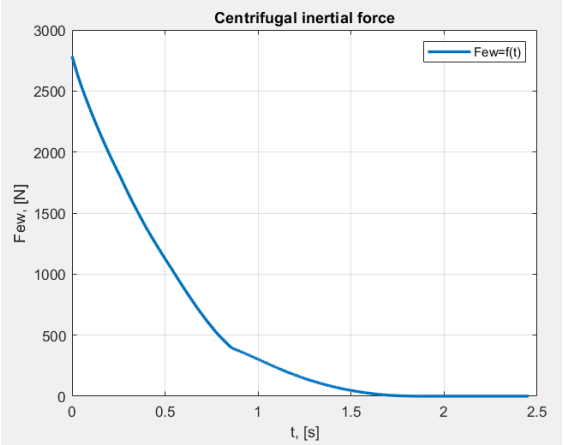

Figure 20. Graphical visualization of the centrifugal inertial force.

During car rotation and the displacement of the body inside the passenger compartment, Coriolis inertial forces are also important. The relative speed to displace the body inside the compartment can be determined according to work–energy theorem, neglecting resistance. It has the following form:

$$\frac{m_p \cdot V_r^2}{2} = \int_{x_o}^{x_1} m_p \cdot \omega_z^2 \cdot x \cdot dx; \;\; V_r = \sqrt{x_1^2 - x_o^2} \cdot \omega \tag{27}$$

where x_1 and x_o are the respective distances from the body center of mass to the vehicle center of gravity at the time of impact and for a given moment while the vehicle is moving.

The Coriolis force has the following magnitude:

$$F_c = 2 \cdot m_p \cdot \omega \cdot V_r = 2 \cdot m_p \cdot \sqrt{x_1^2 - x_o^2} \cdot \omega^2 \tag{28}$$

Coriolis force when displacing the passenger at 0.2 m takes, for example, the following form:

$$F_c = 2 \cdot m_p \cdot \omega \cdot V_r = 2 \cdot 80 \cdot \sqrt{1^2 - 0.8^2} \cdot 5.9^2 = 3342 \text{ N} \tag{29}$$

The net forces generated by the angular velocity, centrifugal forces, Coriolis acceleration and Coriolis forces are as shown below:

$$\vec{F}_{e\omega c} = \vec{F}_{e\omega} + \vec{F}_c \tag{30}$$

The dynamic study at impact shows that the passenger in the front right seat of the car has moved strongly forward and slightly to the right relative to his coordinate system. As a result, the front right door has been massively deformed in the direction of the passenger's body motion. In the subsequent rotational motion around a vertical axis, transfer centrifugal inertial force, which propels the body from passenger compartment, is of primary importance (Figures 21 and 22).

The importance of passive safety systems and, more precisely, the effect of the seat belt in the event of an impact with a stationary barrier is obvious. There are two main directions of motion for the passenger in the front right seat. The first is moving forward and to the right relative to the body's coordinate system, invariably connected to the car's center of mass, and the second is when it is propelled from the passenger compartment through the car's front right door glass. The latter motion results from the action of the sum vector of the centrifugal inertial force and the Coriolis inertial force. The magnitudes of the inertial forces thus obtained determine both the position of the passenger in the car, and the effect of the seat belt on the preservation of the occupant's stable position.

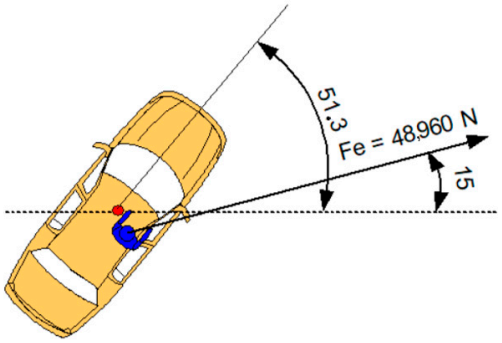

Figure 21. Direction of translation force at impact stage.

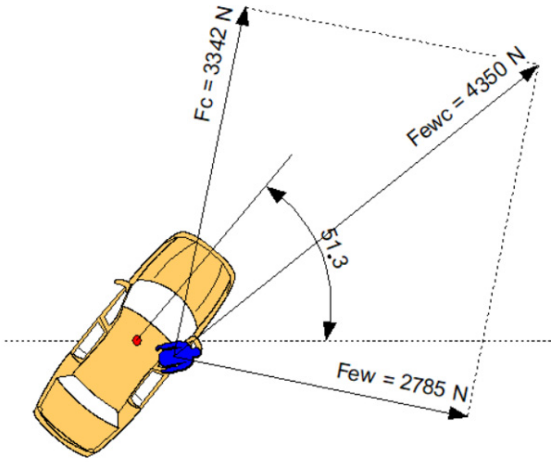

Figure 22. Post-impact direction of centrifugal and Coriolis inertial forces.

4. Conclusions

1. A dynamic study implementing the finite element method using Abaqus/Explicit software product allows for a prediction, with sufficient accuracy, of the impact of the translation inertial forces on the passengers in the car at impact phase in a frontal fixed barrier collision.
2. A mixing problem with differential equations has been solved regarding the dynamics of the impact process when hitting a fixed barrier as well as the post-impact macro motion of the car based on residual kinetic energy.
3. The investigation carried out using the method of finite elements in the impact phase improves the accuracy of data that allow the analysis of the results with precision. This is achieved by taking into account the angular velocity of the car around the vertical axis and the activity of the variable magnitude of the centrifugal inertial force in the impact phase.
4. The effect of the main inertial forces on the impact phase and that of the dominant ones after the impact have been considered, and the maximum magnitude of inertial forces has been predicted with sufficient accuracy.
5. The effect of inertial forces on car occupants in the two main phases—the impact phase and post-impact phase—has been reported.
6. The effect of passive safety systems in the car and the possibility of saving passengers' lives and health in the event of an impact with a stationary barrier have been analyzed.

Author Contributions: Conceptualization, S.K. and H.U.; methodology, H.U.; software, S.D.; data curation, V.U. All authors participated equally in the research. All authors have read and agreed to the published version of the manuscript.

Funding: Please add The APC was founded by the Scientific and Research Sector of the Technical University of Sofia, Bulgaria, IUNF 23000.

Data Availability Statement: Not applicable.

Acknowledgments: The authors would like to thank the Research and Development Sector at the Technical University of Sofia for the financial support.

Conflicts of Interest: The authors declare no conflict of interest.

References

1. Golding, J.; Bles, W.; Bos, J.; Haynes, T.; Gresty, M. Motion Sickness and Tilts of the Inertial Force Environment: Active Suspension Systems vs. Active Passengers. *Aviat. Space Environ. Med.* **2003**, *74*, 220–227. Available online: https://pubmed.ncbi.nlm.nih.gov/12650268/#:~:text=expand-,PMID%3A%2012650268,-Abstract (accessed on 1 May 2023). [PubMed]
2. Fulvio, J.M.; Miao, H.; Rokers, B. Head jitter enhances three-dimensional motion perception. *J. Vis.* **2021**, *21*, 12. Available online: https://www.ncbi.nlm.nih.gov/pmc/articles/PMC7961113/#:~:text=doi%3A%C2%A010.1167/jov.21.3.12 (accessed on 1 May 2023). [CrossRef] [PubMed]
3. Anadu, D.; Mushagalusa, C.; Alsbou, N.; Abuabed, A. Internet of Things: Vehicle collision detection and avoidance in a VANET environment. In Proceedings of the 2018 IEEE International Instrumentation and Measurement Technology Conference (I2MTC), Houston, TX, USA, 14–17 May 2018; pp. 1–6.
4. Zhou, J.; Goodall, R.; Ren, L.; Zhang, H. Influences of car body vertical flexibility on ride quality of passenger railway vehicles. *Proc. Inst. Mech. Eng. Part F J. Rail Rapid Transit.* **2009**, *223*, 461–471. [CrossRef]
5. Kamal, M.M. Analysis and Simulation of Vehicle to Barrier Impact. *SAE Trans.* **1970**, *79*, 1498–1503. Available online: https://www.jstor.org/page-scan-delivery/get-page-scan/44716186/0 (accessed on 5 September 2023).
6. Diana, G.; Cheli, F.; Andrea, C.; Corradi, R.; Melzi, S. The development of a numerical model for railway vehicles comfort assessment through comparison with experimental measurements. *Veh. Syst. Dyn.* **2002**, *383*, 165–183. [CrossRef]
7. Uzunov, H.; Dechkova, S.; Dimitrov, K.; Uzunov, V. Mechanical Mathematical Modelling of a Car Accident Caused by Sudden Mechanical Failure. *J. Eng. Sci. Technol. Rev.* **2021**, *14*, 61–68. Available online: http://www.jestr.org/downloads/Volume14Issue4/fulltext81442021.pdf (accessed on 1 May 2023). [CrossRef]
8. Karapetkov, S.; Dimitrov, L. An Update on the Momentum 360 Method of Vehicle Impact Reconstruction through 3D Modeling and Computer Simulation. *Symmetry* **2022**, *14*, 2628. [CrossRef]
9. Lyubenov, D.; Mateev, V.; Kadikyanov, G. An expert system for vehicle accident reconstruction. *IOP Conf. Ser. Mater. Sci. Eng.* **2019**, *614*, 012006. Available online: https://iopscience.iop.org/article/10.1088/1757-899X/614/1/012006#:~:text=DOI%2010.1088/1757%2D899X/614/1/012006 (accessed on 1 May 2023). [CrossRef]
10. Lyubenov, D.; Balbuzanov, T.; Dinolov, O. Application of GPS-based information system in studying dynamic properties of vehicles. *AIP Conf. Proc.* **2022**, *2570*, 040004. [CrossRef]
11. Karapetkov, S.; Dimitrov, L.; Uzunov, H.; Dechkova, S. Identifying Vehicle and Collision Impact by Applying the Principle of Conservation of Mechanical Energy. *Transp. Telecommun. Riga* **2019**, *20*, 191–204. [CrossRef]
12. Karapetkov, S.; Dimitrov, L.; Uzunov, H.; Dechkova, S. Examination of vehicle impact against stationary roadside objects. In Proceedings of the 9th International Scientific Conference on Research and Development of Mechanical Elements and Systems, IRMES 2019, Code 154497, Kragujevac, Serbia, 5–7 September 2019; University of Kragujevac, Faculty of Engineering Kragujevac: Kragujevac, Serbia, 2019. Available online: https://iopscience.iop.org/article/10.1088/1757-899X/659/1/012063#:~:text=DOI%2010.1088/1757%2D899X/659/1/012063 (accessed on 1 May 2023).
13. Daily, J.; Shigemura, N.; Daily, J. *Fundamentals of Traffic Crash Reconstruction*; Institute of Police Technololgy and Managment, University of North Florida: Jacksonville, FL, USA, 2006; ISBN 978-1-884566-63-9. Available online: https://store.iptm.org/products/fundamentals-of-traffic-crash-reconstruction (accessed on 1 May 2023).
14. Schmidt, B.; Haight, W.; Szabo, T.; Welcher, J. System-based energy and momentum analysis of collisions. In *Accident Reconstruction: Technology and Animation VIII SP-1319, no. 980026*; Society of Automotive Engineers: Warrendale, PA, USA, 1998. [CrossRef]
15. Sharma, D.; Stern, S.; Brophy, J. An Overview of NHTSA's Crash Reconstruction Software WinSMASH. In Proceedings of the Twentieth International Conference on Enhanced Safety of Vehicles, Lyon, France, 18–21 June 2007. Paper No. 07-0211.
16. Prochowski, L.; Ziubiński, M.; Dziewiecki, K.; Szwajkowski, P. Impact energy and the risk of injury to motorcar occupants in the front-to-side vehicle collision. *Nonlinear Dyn.* **2022**, *110*, 3333–3354. Available online: https://link.springer.com/article/10.1007/s11071-022-07779-8 (accessed on 1 May 2023). [CrossRef]
17. Niehoff, P.; Gabler, C. The Accuracy of WinSMASH Delta-V Estimates: The Influence of Vehicle Type, Stiffness, and Impact Mode. *Annu. Proc. Assoc. Adv. Automot. Med.* **2006**, *50*, 73–89. [PubMed]

18. Żuchowski, A. The use of energy methods at the calculation of vehicle impact velocity. In *Wydawnictwo Naukowe Sieci Badawczej Łukasiewicz—Przemysłowego Instytutu Motoryzacji*; Military University of Technology, Faculty of Mechanical Engineering: Warszawa, Poland, 2015; Volume 68, Available online: https://www.infona.pl/resource/bwmeta1.element.baztech-69f9b920-dfe3-40e3-9953-29a4b841aadf (accessed on 1 May 2023).
19. Stronge, W. *Impact Mechanics*; Cambridge University Press: Cambridge, UK, 2000. [CrossRef]
20. Dechkova, S. Creation of multi-mass models in the SolidWorks and Matlab environment for crash identification. *Mach. Mech.* **2018**, *119*, 28–32, ISSN 0861-9727.
21. Kolev, Z.; Kadirova, S. Numerical Modelling of Heat Transfer in Convector's Pipes by ABAQUS. *IOP Conf. Ser. Mater. Sci. Eng.* **2019**, *595*, 012006. Available online: https://iopscience.iop.org/article/10.1088/1757-899X/595/1/012006#:~:text=DOI%2010.1088/1757%2D899X/595/1/012006 (accessed on 1 May 2023). [CrossRef]
22. Kolev, Z.; Kadirova, S. Numerical modeling of the thermal conduction process in water-air convector's fins. *E3S Web Conf.* **2020**, *180*, 01009. [CrossRef]
23. Shelby, S. DELTA-V as a measure of traffic conflict severity. In Proceedings of the 3rd International Conference on Road Safety and Simulation, Indianapolis, IN, USA, 14–16 September 2011. Available online: https://onlinepubs.trb.org/onlinepubs/conferences/2011/RSS/1/Shelby,S.pdf (accessed on 1 May 2023).